RHEUMATOLOGY

Rheumatology 2010;49:1447–1460
doi:10.1093/rheumatology/keq108
Advance Access publication 25 April 2010

Original article

Histone deacetylase inhibitors MS-275 and SAHA induced growth arrest and suppressed lipopolysaccharide-stimulated NF-κB p65 nuclear accumulation in human rheumatoid arthritis synovial fibroblastic E11 cells

Qiu-Yi Choo[1], Paul C. Ho[1], Yoshiya Tanaka[2] and Hai-Shu Lin[1]

Abstract

Objectives. MS-275 and suberoylanilide hydroxamic acid (SAHA) are histone deacetylase (HDAC) inhibitors currently tested in oncology trials. They have also been found to display potent anti-rheumatic activities in rodent models for RA. However, the anti-rheumatic mechanisms of action remain unknown. The study was carried out with the intent of determining the anti-inflammatory and anti-rheumatic mechanisms of the HDAC inhibitors.

Methods. In this study, the anti-rheumatic mechanisms of MS-275 and SAHA were investigated in several cell culture models.

Results. MS-275 and SAHA inhibited human RA synovial fibroblastic E11 cell proliferation in a non-cytotoxic manner. The anti-proliferative activities were associated with G_0/G_1 phase arrest and induction of cyclin-dependent kinase inhibitor p21. In addition, MS-275 and SAHA suppressed lipopolysaccharide (LPS)-induced NF-κB p65 nuclear accumulation, IL-6, IL-18 and nitric oxide (NO) secretion as well as down-regulated pro-angiogenic VEGF and MMP-2 and MMP-9 production in E11 cells at sub-micromolar levels. At similar concentrations, MS-275 and SAHA suppressed LPS-induced NF-κB p65 nuclear accumulation and IL-1β, IL-6, IL-18 and TNF-α secretion in THP-1 monocytic cells. Moreover, NO secretion in RAW264.7 macrophage cells was also inhibited.

Conclusions. In summary, MS-275 and SAHA exhibited their anti-rheumatic activities by growth arrest in RA synovial fibroblasts, inhibition of pro-inflammatory cytokines and NO, as well as down-regulation in angiogenesis and MMPs. Their anti-rheumatic activities may be mediated through induction of p21 and suppression of NF-κB nuclear accumulation.

Key words: Rheumatoid arthritis, Histone deacetylase inhibitor, MS-275, Suberoylanilide hydroxamic acid, NF-κB, p21, Angiogenesis, Metalloproteinase, Nitric oxide, Pro-inflammatory cytokines.

Introduction

Histone deacetylase (HDAC) inhibitors are a new class of anti-cancer agents that have attracted significant interest in drug discovery over the past 10–15 years [1, 2]. Suberoylanilide hydroxamic acid (SAHA or vorinostat) was the first US Food and Drug Administration-approved HDAC inhibitor indicated for cutaneous T-cell lymphoma management [3, 4]. The clinical applications of SAHA in other oncological conditions are currently being tested [5, 6]. There are ~10 more HDAC inhibitors undergoing Phase I–III trials for anti-cancer purposes [5, 6].

Besides anti-neoplastic activities, HDAC inhibitors also exhibited potent anti-inflammatory activities in animal models for inflammatory bowel diseases, multiple sclerosis and SLE [5, 7]. The anti-rheumatic activities of HDAC

[1]Department of Pharmacy, National University of Singapore, Singapore and [2]First Department of Internal Medicine, School of Medicine, University of Occupational and Environmental Health, Kitakyushu, Japan.

Submitted 12 November 2009; revised version accepted 9 March 2010.

Correspondence to: Hai-Shu Lin, Department of Pharmacy, National University of Singapore, 10 Kent Ridge Crescent, Singapore 119260. E-mail: phalh@nus.edu.sg

BASIC SCIENCE

inhibitors have been reported in rodent models for RA [5, 8]. In the first proof-of-concept study, Chung *et al.* [9] found that topical phenylbutyrate (PB) and trichostatin A (TSA) reduced joint swelling, panus formation, subintimal mononuclear cell infiltration, synovial hyperplasia and prevented cartilage or bone destruction in rats with adjuvant-induced arthritis (AIA) [9]. Similarly, TSA suppressed synovial inflammation and cartilage destruction in collagen antibody-mediated arthritic (AMA) mice, while FR235222 (a fungal metabolite with HDAC activities) alleviated joint swelling in AIA rats [10, 11]. Some HDAC inhibitors currently in clinical trials had also been investigated for their potential anti-rheumatic activities. FK-228 (romidepsin; a cyclic tetrapeptide undergoing Phase I–II clinical trials) exhibited potent anti-rheumatic activities in AMA mice and AIA rats [12–14]. In a recent study, *in vivo* anti-rheumatic activities of MS-275 (a benzamide HDAC inhibitor in Phase I–II trials) and SAHA were tested in rodent collagen-induced arthritis (CIA) models [15]. SAHA displayed moderate prophylactic efficacy but could not inhibit CIA onset [15]. However, it alleviated joint swelling and bone erosion in both mice and rats and slightly reduced bone resorption enhanced by arthritis in rats [15]. MS-275 exhibited excellent prophylactic efficacy by preventing bone erosion and markedly delayed CIA onset [15]. Furthermore, disease progression and joint destruction after onset were suspended when MS-275 was used as a therapeutic intervention [15]. Its disease-modifying abilities appeared faster and stronger than MTX, the first-line DMARD used in RA management [15].

Since both MS-275 and SAHA are already in the pipeline for clinical development in oncology, it will be of interest to assess their potential as DMARDs for rheumatology applications. However, the anti-rheumatic mechanisms of MS-275 and SAHA remain unknown. Therefore, we attempted to investigate the anti-rheumatic mechanisms of MS-275 and SAHA in cell culture models in this study. Our results indicate that anti-proliferation of RA synovial fibroblasts (RASFs), inhibition of pro-inflammatory cytokines and nitric oxide (NO), as well as down-regulation of angiogenesis and MMPs can contribute to the anti-rheumatic activities of HDAC inhibitors. Such anti-rheumatic activities may be mediated through induction of p21 and suppression of NF-κB nuclear accumulation.

Materials and methods

HDAC inhibitors

MS-275 (purity >95%) and SAHA (purity >98%) were purchased from Axxora (San Diego, CA, USA) and Toronto Research Chemicals (North York, Canada), respectively. MS-275 was dissolved in dimethyl sulfoxide (DMSO) (MP Biomedicals, Solon, OH, USA) to obtain a stock solution of 50 mM and SAHA was dissolved in a solution containing 0.3% (w/v) of sodium hydroxide in 0.9% (w/v) of sodium chloride, to obtain a stock solution of 25 mM. The stock solutions were stored at −20°C. They were diluted to required concentrations in subsequent experiments with growth media.

Cell lines and cell culture

E11 is a cell line developed from human RASFs [16, 17]. Human monocytic cell line THP-1 (TIB-202) and murine macrophage cell line RAW264.7 (TIB-71) were purchased from American Type Culture Collection (ATCC; Manassas, VA, USA). E11 cells were grown in Roswell Park Memorial Institute (RPMI) 1640 medium (Invitrogen, Carlsbad, CA, USA) supplemented with 10% (v/v) heat-inactivated fetal bovine serum (FBS; HyClone, Waltham, MA, USA). THP-1 cells were also cultured in RPMI 1640 medium, in the presence of 20% FBS and 0.05 nM 2-mercaptoethanol (Sigma-Aldrich, St Louis, MO, USA). RAW264.7 cells were cultured in DMEM (Invitrogen) with 10% FBS. One per cent (v/v) antibiotic–anti-mycotic solution (Invitrogen) was added to all culture media to prevent contamination. All cell cultures were maintained at 37°C in a humidified atmosphere with 5% CO_2.

E11 cell proliferation assay

E11 cell proliferation was assessed by dimethylthiazol tetrazolium bromide (MTT) assay in accordance with an ATCC protocol [18]. Briefly, E11 cells (0.5×10^6 cells/well) were seeded in 24-well flat-bottom plates and incubated for 24 h before various concentrations of HDAC inhibitors or MTX (Sigma-Aldrich) were added (final concentrations: 2.5 nM to 25 μM). The medium was aspirated after 72 h and cells were washed with phosphate buffer solution (PBS) before 200 μl of MTT (Sigma-Aldrich) was added (final concentration: 50 μg/ml). The cells were incubated for at least 4 h at 37°C. Formazan formed was solubilized with DMSO (MP Biomedicals) and the levels determined by measuring optical densities (ODs) with Genios plate reader (Tecan Group, Männedorf, Switzerland) at 570 nm. Cell proliferation was expressed as percentage cell growth with respect to control cells, from which proliferation inhibition was calculated.

Cytotoxicity

In an initial study, E11 cell viability was assessed by trypan blue exclusion method after 72-h incubation with HDAC inhibitors or MTX at two concentrations (a low concentration of 50 nM and a high concentration of 5 μM). In later studies, the cytotoxicity of HDAC inhibitors and MTX were further investigated using a Cytotoxicity Detection Kit (Roche Applied Science, Indianapolis, IN, USA), which is dependent on lactate dehydrogenase (LDH) released from the cytosol of dead cells into the media. Briefly, E11 cells were maintained in RPMI 1640 supplemented with 1% FBS, 1% antibiotic–anti-mycotic solution and incubated at 37°C with 5% CO_2 before seeding in 96-well flat-bottom plates and incubated for 24 h before various concentrations of HDAC inhibitors or MTX were added (final drug concentrations: 2.5 nM to 25 μM). The medium was aspirated after 72 h and retained for cytotoxicity analyses, in accordance with the manufacturer's

instructions. Optical densities were read with a Genios plate reader (Tecan Group) at 490 nm with a reference wavelength of 620 nm.

Cell cycle distribution analysis

The cell cycle distribution of E11 cells was also examined. Briefly, E11 cells were seeded in 25-mm^3 culture flasks and incubated for 24 h before various concentrations of HDAC inhibitors (final concentrations: 1 nM to 1 μM) were added and incubated overnight. After 24 h, cells were trypsinized and washed twice with PBS. They were then fixed by resuspending the cell pellet in ice-cold 70% (w/w) ethanol overnight. Before analyses, cell suspensions were washed twice with PBS before resuspending in a staining buffer [50 μg/ml of propidium iodide (PI; Sigma-Aldrich) and 70 U RNase (Sigma-Aldrich) in 100 ml PBS] and incubated for at least 1 h in the dark at room temperature [19]. Cell cycle distribution was visualized using Coulter Elite Flow Cytometer (Beckman Coulter, Fullerton, CA, USA). Histograms were analysed with Summit version 4.3 (Dako, Glostrup, Denmark).

Expression of cyclin-dependent kinase inhibitors p16, p21 and p27

E11 cells were seeded in 6 cm Petri dishes and incubated for 24 h before HDAC inhibitors were added (final concentration: 50 nM). At stipulated time intervals, samples were harvested. The medium was aspirated and cells were washed with ice-cold PBS before being scraped off the culture dish. They were treated with 100 μl of lysis buffer (1% Triton X-10, protease inhibitor and 50 mM Tris–HCl pH 7.4). After 30 min of lysis on ice, the samples were centrifuged at 1100 *g* for 10 min at 4°C. Proteins in the supernatant were separated by SDS–PAGE using a (×2) SDS loading buffer [0.02% bromophenol blue, 0.2 M dithiothreitol (DTT), 20% glycerol, 8% SDS and 0.25 M Tris–HCl pH 6.8]. The proteins loaded were equalized using bicinchoninic acid (BCA) assay (Pierce Biotechnology, Rockford, IL, USA) and resolved by a 12.5% SDS–PAGE gel at 150 V for 45 min.

Following electrophoresis, separated proteins were transferred to polyvinylidene fluoride or nitrocellulose membranes in a transfer buffer (192 mM glycine, 20% methanol and 25 mM Tris–HCl pH 8) at a constant voltage of 125 V for 1 h at 4°C in an electro-transfer unit (Bio-Rad Laboratories, Hercules, CA, USA). Membranes were then incubated in 2% (w/v) solution of non-fat milk dissolved in PBS (MPBS) for 1 h at room temperature. They were probed with primary antibodies against p16, p21, p27 and β-actin (Santa Cruz Biotechnology, Santa Cruz, CA, USA), which were diluted in 3% BSA. The membrane was left overnight at 4°C. Subsequently, it was washed thrice with PBS before incubation for 1 h at room temperature with secondary antibodies (peroxidase conjugated ImmunoPure goat anti-mouse IgG or goat anti-rabbit IgG; Pierce Biotechnology) diluted in 2% (w/v) MPBS. Thereafter, the membrane was washed thrice with PBS. SuperSignal West Pico Chemiluminescent Substrate (Pierce Biotechnology) was added to the membrane and resultant signals were detected by exposure to MultImage Light Cabinet (Alpha Innotech, San Leandro, CA, USA).

NF-κB p65 protein nuclear accumulation

The nuclear level of NF-κB p65 protein was assessed by an ELISA kit from Active Motif (Carlsbad, CA, USA). Briefly, E11 or THP-1 cells (1×10^6 cells/flask) were seeded in 25-mm^3 culture flasks for 24 h before HDAC inhibitors of varying concentrations were added (final concentrations: 100–1000 nM). After 1 h, lipopolysaccharide (LPS; Sigma-Aldrich) was added (final concentration: 5 μg/ml) and incubated for another 24 h. The NF-κB p65 in the nuclear extracts was quantified by ELISA in accordance with manufacturer's instructions. Care was taken to ensure that extracts used gave OD_{260} : OD_{280} ratio in the range 1.8–2.0. Optical densities were determined by a Genios plate reader (Tecan Group) at 450 nm and a reference wavelength of 655 nm.

Association between NF-κB and p300 protein

The association between NF-κB and p300 protein, a well-known acetyltransferase, was also examined with a universal magnetic co-immunoprecipitation (Co-IP) kit (Active Motif). Briefly, E11 cells were seeded in 25-mm^3 flasks and incubated for 24 h before HDAC inhibitors (final concentration: 50 nM) were added and incubated for another 24 h before harvesting. The cells were lysed and the nuclear extract was immunoprecipitated with antibody to p300 (Santa Cruz Biotechnology). The immunoprecipitants were immunoblotted with antibody to NF-κB p65 (Santa Cruz Biotechnology) and fractionated by SDS–PAGE. Bands were visualized by MultImage Light Cabinet.

Distribution of acetylated NF-κB p65 protein

The distribution profile of acetylated NF-κB p65 protein was also investigated. Briefly, E11 cells were seeded in 25-mm^3 flasks and incubated for 24 h before HDAC inhibitors (final concentration: 50 nM) were added. Both nuclear and cytoplasmic fractions were extracted using the universal magnetic CO-IP kit from Active Motif. Cells were lysed and immunoprecipitated with antibody to acetylated NF-κB p65 (against acetylated lysine residue 310; Abcam, Cambridge, MA, USA). The immunoprecipitants were immunoblotted with antibody to acetylated NF-κB (Abcam) and fractionated by SDS–PAGE. Bands were visualized by MultImage Light Cabinet.

NO secretion

The secretion of NO was monitored in both E11 and RAW264.7 cells using an established colorimetric method [20]. E11 or RAW264.7 cells were seeded in 24-well flat-bottom plates and incubated for 24 h before varying concentrations of HDAC inhibitors were added (final drug concentrations: 1–2500 nM). After 1 h, LPS

was added (final concentration 5 μg/ml) and incubated for another 24 h. Accumulation of nitrite [an indicator of NO synthase (NOS) activity] in the supernatant was determined using Griess reagent (Sigma-Aldrich). One hundred microlitres of the supernatant was mixed with an equal volume of Griess reagent at room temperature for 10 min. Thereafter, the optical densities were measured with a Genios plate reader (Tecan Group) at 540 nm. Sample nitrite concentrations were calculated with respect to an external standard of sodium nitrite (Sigma-Aldrich) in the range 1–100 μM.

RT–PCR analysis for cyclo-oxygenase-2 and inducible NOS transcription in E11 cells

E11 cells were seeded in 25-mm^3 flasks and incubated for 24 h before HDAC inhibitors (final concentration: 100 nM) were added. After 1 h, LPS (final concentration: 5 μg/ml) was added and incubated for another 24 h. RNA was extracted using RNeasy mini kit (Qiagen, Germantown, MD, USA). First-strand cDNA was manufactured using RevertAid First Strand cDNA Synthesis Kit (Fermentas Life Science, Berlington, Canada). Single-strand cDNA was then amplified into mRNA. The primers used were from First Base, Singapore:

Cyclo-oxygenase-2 (COX-2):
5′-GGTCTGGTGCCTGGTCTGATGATG-3′ (sense)
5′-GTCCTTTCAAGGAGAATGGTGC-3′ (anti-sense)
Inducible NOS (iNOS):
5′-ATGCCAGATGGCAGCATCAGA-3′ (sense)
5′-TTTCCAGGCCCATTGTCCTGC-3′ (anti-sense)
Glyceraldehyde-3-phosphate dehydrogenase (GAPDH):
5′-TGATGACATCAAGAAG GTGGTGAAG-3′ (sense)
5′-TCCTTGGAGGCCATGTGGGCCAT-3′ (anti-sense)

RT–PCR analyses for COX-2 were performed with its primers in a 25-μl reaction mixture (2.5 U of AmpliTaq DNA polymerase, 0.2 mM dNTP, 50 mM KCl, 2 mM $MgCl_2$, 1 μg of cDNA, 400 nM primers and 10 mM Tris buffer pH 8.3) for 35 cycles consisting denaturation at 94°C for 20 s, annealing at 52°C for 20 s, extension at 72°C for 30 s and final extension at 72°C for 10 min. The conditions for iNOS were identical to COX-2, except for annealing at 55°C. A constitutively expressed gene, GAPDH, was used as internal control.

Resultant mRNA was mixed with loading dye and resolved using a 0.1% (w/v) agarose gel at 80 V for 1 h. After which, it was incubated with ethidium bromide (Bio-Rad) for 15 min before visualizing with Gel Doc XR system (Bio-Rad). Band densitometry was performed using ImageJ Version 1.42 [21]. Relative intensities of treatment bands with respect to control bands were obtained by comparing the intensities of bands obtained from cells treated with LPS and HDAC inhibitors with that from control cells.

Cytokine secretions

ELISA sets for human IL-1β, IL-6 and TNF-α were purchased from BD Biosciences (San Jose, CA, USA). ELISA set for human IL-18 was obtained from Bender MedSystems (Vienna, Austria). E11 cells were seeded in 24-well flat-bottom plates and incubated for 24 h before varying concentrations of HDAC inhibitors were added (final concentrations: 1–1000 nM). Hydrocortisone sodium succinate (HYD; Pharmacia, Puurs, Belgium; final concentration: 1 μM) served as positive control. After 1 h, LPS was added (final concentration: 5 μg/ml) to stimulate the secretions of pro-inflammatory cytokines. Twenty-four hours later, the media were harvested and the cytokine levels were quantified with ELISA. As E11 cells had high baseline expression of IL-6 [22], LPS stimulation was not required when assessing the impact of HDAC inhibitors on IL-6 secretion. Moreover, the LPS-stimulated secretions of IL-1β, IL-6, IL-18 and TNF-α were also monitored in THP-1 cells. Optical densities for IL-1β, IL-6 and TNF-α were read with Genios plate reader (Tecan Group) at 450 nm with a reference wavelength of 570 nm, whereas that for IL-18 was read at 450 nm with a reference wavelength of 620 nm. To investigate the impact of NF-κB in the secretions of these inflammatory cytokines, the effects of BAY 11-7082 (Sigma-Aldrich), a well-known NF-κB inhibitor [23, 24], at 1, 2.5 and 5 μM was also investigated.

VEGF secretion

The secretion of VEGF from E11 cells was assessed with ELISA (Bender MedSystems). Briefly, E11 cells were seeded in 24-well flat-bottom plates and incubated for 24 h before varying concentrations of HDAC inhibitors (final concentrations: 1–1000 nM) or HYD (final concentration: 1 μM) were added. After 1 h, the cells were incubated with a combination of IL-6 (final concentration: 100 ng/ml), soluble IL-6 receptor (sIL-6R; final concentration: 100 ng/ml) and IL-1β (final concentration: 5 ng/ml) for another 24 h [25]. VEGF secreted into supernatant was quantified using ELISA. Optical densities were read with a Genios plate reader (Tecan Group) at 450 nm and a reference wavelength of 620 nm.

Gelatin gel zymography assay for gelatinase A (MMP-2) and gelatinase B (MMP-9) secretion from E11 cells

E11 cells were seeded in 25-mm^3 culture flasks and incubated for 24 h before HDAC inhibitors (final concentration: 100 nM) were added. After 1 h, LPS (final concentration 5 μg/ml) was added and incubated for another 30 min. One part of the medium was mixed with one part of sample buffer (0.1% bromophenol blue, glycerol, 10% SDS and 0.5 M Tris–HCl pH 6.8) and allowed to stand for 10 min at room temperature. The amount of proteins in the supernatant used were equalized using BCA assay (Pierce Biotechnology). Samples were mixed with an (×2) SDS loading buffer (0.02% bromophenol blue, 0.2 M DTT, 20% glycerol, 10% SDS and 0.25 M Tris–HCl pH 6.8). Subsequently, they were resolved by a 10% SDS–PAGE gel, containing 0.2% (w/v) gelatin (Sigma-Aldrich) at 100 V for 1 h. After the run, the gel was incubated with a renaturing buffer (25% Triton-X in PBS) and gently agitated for 1 h at room temperature. Then, the

renaturing buffer was decanted and replaced with developing buffer (5 mM $CaCl_2$, 200 mM NaCl and 50 nM Tris–HCl pH 7.4). The gel was equilibrated in developing buffer for 30 min at room temperature with gentle agitation before replacement with fresh developing buffer and incubation overnight at 37°C. It was later stained with Coomassie blue 0.5% (w/v) (Bio-Rad) for 30 min before destaining with acetic acid, methanol and water (10 : 50 : 40). Areas of protease activity would appear as clear bands against a dark background where proteases had digested gelatin.

Data analysis and statistics

GraphPad Prism 5 (GraphPad Software, La Jolla, CA, USA) was used in statistical analyses and the calculation for 50% inhibitory concentration (IC_{50}). Since only parametric data existed in this study, two-tailed unpaired *t*-test was applied. $P < 0.05$ was considered to be statistically significant.

Results

MS-275 and SAHA induced growth arrest in E11 cells in a cytotoxicity-independent manner

In order to determine if HDAC inhibitors affect cell proliferation, the growth inhibitory effects of MS-275 and SAHA in E11 cells were examined by MTT assay. MTX, the first-line DMARD for RA, was used as a positive control. MS-275, SAHA or MTX inhibited E11 cell proliferation dose dependently. They had comparable potencies (Fig. 1A). Interestingly, the effective levels for MS-275 and SAHA to suppress E11 cell proliferation were fairly low and the IC_{50} values were <100 nM (Table 1). In contrast, the IC_{50} values of MS-275 and SAHA in cancer cell lines were often observed to be >1 μM [1, 5].

In order to rule out cytotoxicity in the anti-proliferative results, E11 cells treated with MS-275, SAHA and MTX were examined with trypan blue exclusion under the microscope. Incubation of E11 cells with 5 μM MS-275 or SAHA for 72 h did not cause significant cell death (cell viability >95%). However, MTX resulted in significant E11 cell cytotoxicity. At 50 nM and 5 μM, the cell viability was 80 and 40%, respectively.

As counting of cells in trypan blue exclusion may be subjective, we confirmed our results with LDH assays. Neither MS-275 nor SAHA increased LDH release into cell culture media compared with control, even at 25 μM (Fig. 1B). In contrast, MTX displayed concentration-dependent cytotoxicity. It elevated LDH activity significantly ($P < 0.01$) even at 10 nM. Therefore, the anti-proliferative activity of MTX was associated with cytotoxicity, whereas that of MS-275 and SAHA was not.

Since anti-proliferative effects of HDAC inhibitors were not due to cytotoxicity, cell cycle phase changes were suspected. The impact of MS-275 and SAHA on cell cycle distribution was then investigated. MS-275 or SAHA treatment over the tested range did not significantly increase the sub-G_1 peak, confirming that they did not cause apoptosis (Fig. 1C). However, phase arrest at G_0/G_1 was observed even at a concentration as low as 1 nM. After 24-h incubation with 1 nM MS-275, the G_0/G_1 fraction was increased from 50.1% (1.0%) to 61.4% (2.7%) [mean (S.D.), $P < 0.001$, $n = 5$]. Similarly, a 24-h incubation with 1 nM SAHA caused the G_0/G_1 fraction to increase from 49.1% (1.6%) to 68.1% (0.8%) [mean (S.D.), $P < 0.001$, $n = 5$]. Phase arrest appeared to be concentration independent as increases in MS-275 or SAHA concentrations did not further alter the phase distribution patterns.

As MS-275 and SAHA induced growth arrest at G_0/G_1 phase, it was of interest to determine if the aforementioned observations were attributable to their impact on cyclin-dependent kinase (CDK) inhibitors such as p16, p21 and p27, which play important roles in cell cycle control [26]. Moreover, it had been demonstrated that HDAC inhibitors could up-regulate the expression of these proteins and this is one of the common anti-cancer mechanisms of HDAC inhibitors [1, 2]. To assess the impact of MS-275 and SAHA on p16, p21 and p27 expression, E11 cells were incubated with 50 nM of MS-275 or SAHA (a concentration close to their anti-proliferation IC_{50} value) up to 24 h. Expression levels of p16, p21 and p27 were then monitored by western blot. It was found that E11 cells had high background levels of p16 and p27 but MS-275 or SAHA did not have a significant impact on their expression (western blotting data not shown). MS-275 and SAHA could, however, induce the expression of p21 after 24 h incubation (Fig. 1D).

NF-κB inhibitor BAY 11-7082 suppressed pro-inflammatory cytokine secretions in E11 and THP-1 cells

NF-κB plays an important role in RA pathogenesis and activation of NF-κB leads to expression of various pro-inflammatory cytokines [27–29]. Therefore, we used BAY 11-7082, a well-known NF-κB inhibitor to investigate whether NF-κB blockage offered anti-inflammatory activities.

IL-6 and IL-18 are two pro-inflammatory cytokines involved in RA pathogenesis [30]. As they are expressed in RASFs [30, 31], we measured their secretions from E11 cells with ELISA. We confirmed that E11 cells had fairly high baseline secretion of IL-6 and IL-18 into the cell culture media (about 7000 and 1500 pg/ml, respectively). LPS did not have a significant impact on IL-6 secretion but it up-regulated IL-18 secretion by ~30% compared with control cells (data not shown). BAY 11-7082 suppressed IL-6 and IL-18 secretions from E11 cells concentration dependently. At 1, 2.5 and 5 μM, BAY 11-7082 inhibited IL-6 by 68.2% (2.2%), 80.5% (1.9%), 86.8% (1.0%) [mean (S.D.), $n = 4$], respectively. Similarly, it suppressed IL-18 by 65.5% (1.3%), 78.0% (1.6%), 84.3% (1.7%) [mean (S.D.), $n = 4$], respectively.

THP-1 cells did not possess much baseline IL-1β, IL-6 and TNF-α. However, the secretion of these pro-inflammatory cytokines was boosted after LPS addition

Fig. 1 Anti-proliferative activities of MS-275 and SAHA in E11 cells. (**A**) E11 cells were incubated with MS-275, SAHA or MTX at different concentrations. Proliferation was assessed by MTT assay ($n = 6$). (**B**) E11 cells were incubated with MS-275, SAHA or MTX at different concentrations. Cytotoxicity was monitored by measuring LDH released from the cytosol of dead cells into the media ($n = 6$). The OD_{490} values present the LDH activities in cell culture media. Medium alone (−); positive control (+) (cells treated with 1% Triton X-100). (**C**) After incubation with MS-275 or SAHA at various concentrations overnight, E11 cells were harvested and the cell cycle distribution was analysed with flow cytometry ($n = 5$). Bars show the mean (S.D.) in (**A–C**). $^{**}P < 0.01$ *vs* the vehicle control, $^{***}P < 0.001$ *vs* the vehicle control, by two-tailed unpaired *t*-test. (**D**) After incubation with MS-275 or SAHA (50 nM) for 0, 2, 8 or 24 h, E11 cells were harvested and the expression of p21 was analysed by western blotting. The gel sections were obtained from different gels for each tested antibody, as indicated by the dividing lines.

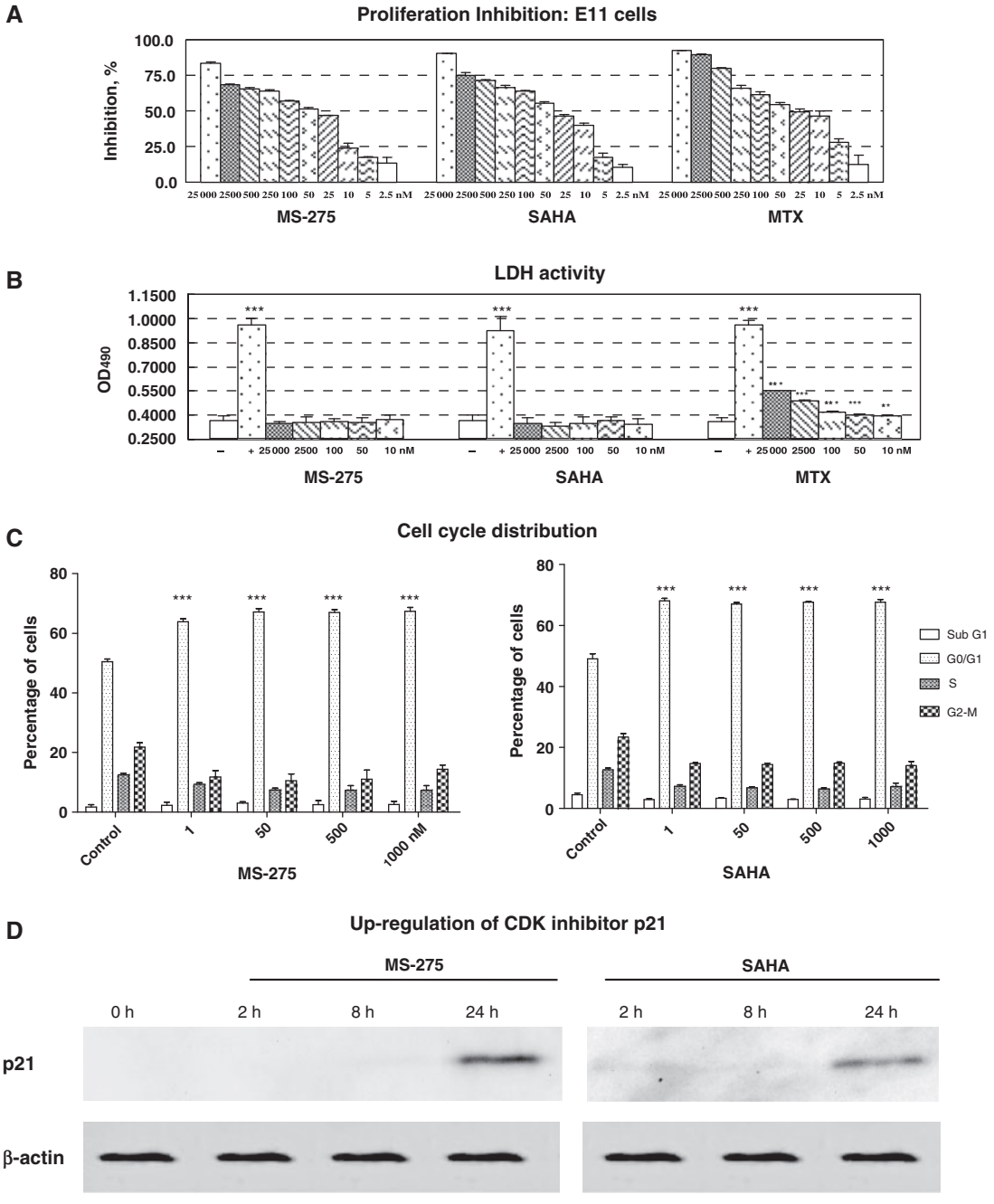

Table 1 IC_{50} values (nM) of MS-275 and SAHA

Cell	Activity	MS-275	SAHA
E11	Proliferation	65	44
E11	NF-κB activation	<100	<100
E11	NO production	<1	<1
E11	IL-6 secretion	121	5311
E11	IL-18 secretion	<1	<1
E11	VEGF secretion	5	62
THP-1	NF-κB activation	<100	<100
THP-1	TNF-α	8	53
THP-1	IL-1β	34	101
THP-1	IL-6	20	51
THP-1	IL-18	<1	<1
RAW264.7	NO production	20	45

compared with control cells. BAY 11-7082 exhibited concentration-dependent suppression on these pro-inflammatory cytokines. At 1, 2.5 and 5 μM, it inhibited IL-1β by 76.2% (2.2%), 82.7% (1.7%), 93.6% (1.3%) [mean (S.D.), $n = 4$], respectively; inhibited IL-6 by 73.3% (2.2%), 86.0% (2.0%), 92.4% (1.0%) [mean (S.D.), $n = 4$], respectively; inhibited IL-18 by 83.0% (2.2%), 92.4% (1.0%), 95.5% (1.9%) [mean (S.D.), $n = 4$], respectively; and inhibited TNF-α by 65.8% (2.2%), 72.3% (1.9%), 83.3% (1.5)% [mean (S.D.), $n = 4$], respectively. Clearly, blockade of NF-κB pathway displayed anti-inflammatory activities in both RASFs and monocytes.

MS-275 and SAHA inhibited LPS-induced NF-κB p65 protein nuclear accumulation and increased association between NF-κB and p300

As NF-κB plays an important role in RA pathogenesis [27–29], it was of interest to assess the impact of MS-275 and SAHA on NF-κB. The inhibitory effects of MS-275 and SAHA on NF-κB nuclear accumulation were observed in E11 cells (Fig. 2A). The baseline level of NF-κB p65 in nuclear extracts of control cells was minimal. LPS enhanced the nuclear accumulation of NF-κB p65 by ~15-fold. However, in the presence of MS-275 or SAHA at 100 nM, ~75% of the observed nuclear accumulation was inhibited. Hence, MS-275 and SAHA effectively inhibited NF-κB p65 nuclear accumulation in E11 cells at concentrations close to their anti-proliferative IC_{50} values. However, further increases in the concentration of MS-275 or SAHA to 500 or 1000 nM, respectively, did not substantially suppress NF-κB p65 nuclear accumulation further.

In order to determine whether NF-κB interacted with transcription co-activator p300, the nuclear extract of E11 cells was immunoprecipitated with p300 antibody and immunoblotted with NF-κB p65 antibody. It was also confirmed that NF-κB p65 formed a complex with p300 transcription co-activator in E11 cells (Fig. 2B). Moreover, MS-275 and SAHA increased the association between p300 and NF-κB p65 (Fig. 2B).

In order to confirm the inhibitory effect of MS-275 and SAHA on NF-κB p65 nuclear accumulation, the distribution profile of acetylated NF-κB within the nucleus and cytoplasm was assessed with Co-IP. There was little acetylated NF-κB in either the nucleus or cytoplasm of control cells. LPS increased acetylated NF-κB localization in the nucleus. There was less acetylated NF-κB p65 in the nuclear fraction as compared with the cytoplasmic fraction when the cells were treated with MS-275 and SAHA. The aforementioned is in line with results obtained from the NF-κB ELISA study that MS-275 and SAHA were able to reduce NF-κB p65 nuclear accumulation significantly. The effects of HDAC inhibitors on acetylated NF-κB p65 localization in E11 cells are shown in Fig. 2C.

MS-275 and SAHA suppressed NO secretion in E11 and RAW264.7 cells

NO appears to be a pro-inflammatory chemokine in RA [5]. E11 cells had very high baseline NO secretion (~250 μM) and LPS could only increase NO secretion by ~1-fold compared with control cells (data not shown). Both MS-275 and SAHA inhibited NO dose dependently (Fig. 3A) with superior potency. NO secretion was inhibited by >50% even at 1 nM. The inhibitory effects of MS-275 and SAHA on NO were also assessed in RAW264.7 cells. Similar to the results observed in E11 cells (Fig. 3A), both MS-275 and SAHA inhibited NO dose dependently at sub-micromolar levels (Table 1).

Since MS-275 and SAHA inhibited NO secretion, it was of interest to determine if it was due to modulation in iNOS expression. iNOS was found to be expressed in E11 cells constitutively and LPS could enhance its transcription. MS-275 and SAHA worked at the transcriptional level to inhibit iNOS expression (Fig. 3B). The results were in good accord with the NO secretion data (Fig. 3A). Similarly, COX-2 was also expressed in E11 cells and LPS increased its transcription. However, only MS-275 was able to decrease its transcription.

MS-275 and SAHA suppressed IL-6, IL-18, VEGF secretion and down-regulated MMP-2 and MMP-9 in E11 cells

MS-275 and SAHA suppressed IL-6 and IL-18 in a concentration-dependent manner (Fig. 4A and B). Noteworthy, IL-18 secretion was more sensitive to HDAC inhibitor treatment as secretion was inhibited by >50% with 1 nM of MS-275 or SAHA. HYD, a clinically active anti-inflammatory glucocorticoid, inhibited the secretion of IL-6 and IL-18 by ~50% compared with control cells at 1 μM (data not shown).

Angiogenesis is also involved in RA pathogenesis [5, 31]. As VEGF is a key regulator of angiogenesis and is expressed in RASFs [30, 31], the impact of MS-275 and SAHA on VEGF was also investigated in E11 cells. The secretion of VEGF from E11 was stimulated by a combination of IL-6, sIL-6R and IL-1β. Both MS-275 and SAHA inhibited VEGF secretion in a concentration-dependent manner (Fig. 4C). Interestingly, at 1 nM, they exhibited potencies ranging from 30 to 40% inhibition. The aforementioned was only achieved by HYD at 1 μM (data not shown).

Fig. 2 MS-275 and SAHA-inhibited NF-κB signalling. (**A**) E11 cells were incubated with MS-275 or SAHA at various concentrations for 1 h. NF-κB p65 nuclear accumulation was stimulated by LPS. Twenty-four hours later, NF-κB p65 nuclear accumulation was quantified by an ELISA kit ($n = 4$). The OD_{450} values represent the nuclear levels of p65. Medium alone (−); positive control (+) from the kit (Raji nuclear extract, Active Motif, Carlsbad, CA, USA), LPS: LPS alone; ***$P < 0.001$ *vs* the LPS alone, by two-tailed unpaired *t*-test. (**B**) E11 cells were incubated with MS-275 or SAHA (50 nM) for 1 h. NF-κB p65 nuclear accumulation was stimulated by LPS. Twenty-four hours later, the nuclear extract was immunoprecipitated with p300 antibody. NF-κB p65 associated with p300 was visualized by western blotting. (**C**) E11 cells were incubated with MS-275 or SAHA (50 nM) for 1 h. NF-κB p65 nuclear accumulation was stimulated by LPS. The nuclear and cytoplasmic extracts were immunoprecipitated with antibody specific to lysine residue 310 on acetylated NF-κB p65. The distribution profile of acetylated NF-κB p65 between nuclei and cytoplasm was visualized by western blotting. The gel sections were taken from different gels for each tested antibody, as indicated by the dividing lines.

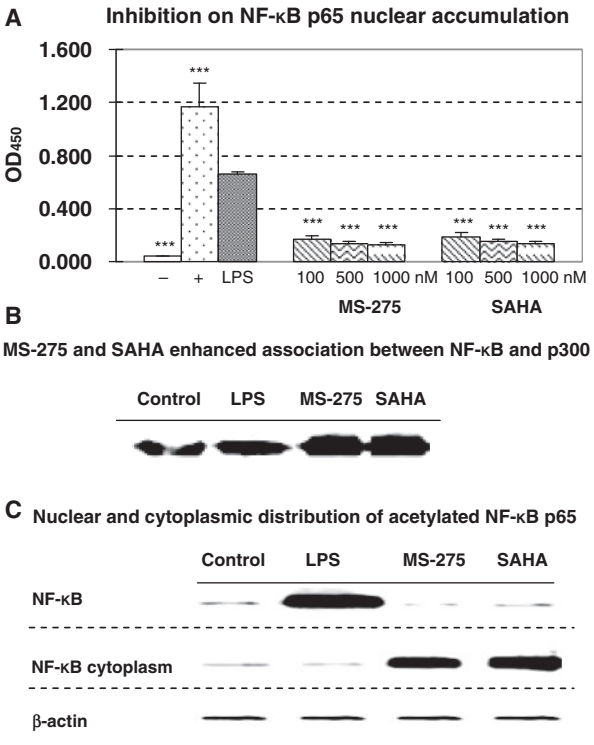

MMPs play an important role in cartilage damage and joint destruction in RA [31]. Elevated levels of MMP-2 and MMP-9 have been reported in SF [32, 33]. The secretion of MMP-2 and MMP-9 in E11 cells was investigated using gelatin zymography. As shown in Fig. 4D, E11 cells secreted both MMP-2 and MMP-9 in pro form (pro-MMP-2 or pro-MMP-9) as well as active form. The activity of pro-MMP-2 was observed to be more abundant. LPS stimulation did not alter the secretion of MMP-2 or MMP-9 as compared with control cells. However, MS-275 and SAHA (100 nM) significantly reduced the activities of pro-MMP-2, pro-MMP-9, MMP-2 and MMP-9. The pro-MMP-2 and MMP-9 bands became nearly invisible after treatment with MS-275 or SAHA. Hence, MS-275 and SAHA were able to down-regulate MMP-2 and MMP-9 production.

MS-275 and SAHA suppressed LPS-induced pro-inflammatory cytokine secretion in THP-1 cells

The inhibitory effects on NF-κB p65 nuclear accumulation were also assessed in THP-1 cells. Similar to the results observed in E11 cells (Fig. 2A), MS-275 or SAHA (100 nM) inhibited ~70% of the p65 nuclear accumulation (data not shown). Both MS-275 and SAHA suppressed IL-1β, IL-6, IL-18 and TNF-α in a concentration-dependent manner (Fig. 5A–D). The suppression was achievable at sub-micromolar levels (Fig. 5A–D and Table 1). In comparison, HYD (1 μM) suppressed IL-1β, IL-6, IL-18 and TNF-α secretion, by 85, 40, 60 and 80%, respectively (data not shown).

Discussion

The role of histone acetylation in RA pathogenesis is unclear. Huber *et al.* [34] reported that the activity of histone acetyltransferase remained unchanged in the synovial tissues of OA, RA or arthritis-free controls, while HDAC activity was significantly suppressed in both OA and RA compared with controls. Controversially, Horiuchi *et al.* [35] found that the mRNA level of HDAC1 was significantly higher in RASFs than in osteoarthritic synovial fibroblasts (OASFs). Moreover, knockdown of HDAC1 and HDAC2 resulted in decreased cell counts and cell proliferation, and increased apoptosis in RASFs [35]. Further studies are required to elucidate the relationship between histone acetylation and RA pathogenesis.

As SFs play an important role in RA pathogenesis and work actively to drive joint destruction [31, 36, 37], we investigated the anti-rheumatic mechanisms of MS-275 and SAHA in E11 cells, a cell line developed from RASFs [16, 17]. RASFs differed from normal SFs and OASFs [5]. However, RASFs shared many similarities with neoplastic tissues, including anchorage-independent growth, extensive proliferation and loss of contact inhibition, impaired apoptosis or senescence, somatic gene mutations and extensive angiogenesis, monoclonal or oligoclonal expansion and oncogene activation [5, 37, 38]. As RASFs share common characteristics with malignant tissues, some anti-cancer drugs, such as MTX, offer therapeutic benefits in RA. HDAC inhibitors are a new family of anti-cancer agents currently undergoing extensive clinical investigations. They are well known for their anti-proliferative and apoptosis/differentiation-inducing activities in cancer cells [5, 6]. Therefore, HDAC inhibitors could potentially be effective for RA treatment. Furthermore, the *in vivo* anti-rheumatic efficacies of

FIG. 3 MS-275 and SAHA suppressed NO secretion. (**A**) E11 or RAW264.7 cells were incubated with MS-275 or SAHA at different concentrations. NO secretion was stimulated with LPS and measured by Griess reagent ($n = 6$). Predicted values (——), observed values (•) of MS-275 on NO inhibition; predicted values (- - -), observed values (○) of SAHA on NO inhibition. Bars show the mean (S.D.) in (**A**). (**B**) E11 cells were incubated with MS-275 or SAHA (100 nM). COX-2 and iNOS transcription was stimulated with LPS and assessed by RT–PCR. The gel sections were taken from different parts of the same gel, as indicated by the dividing lines. Control: medium alone; LPS: LPS alone.

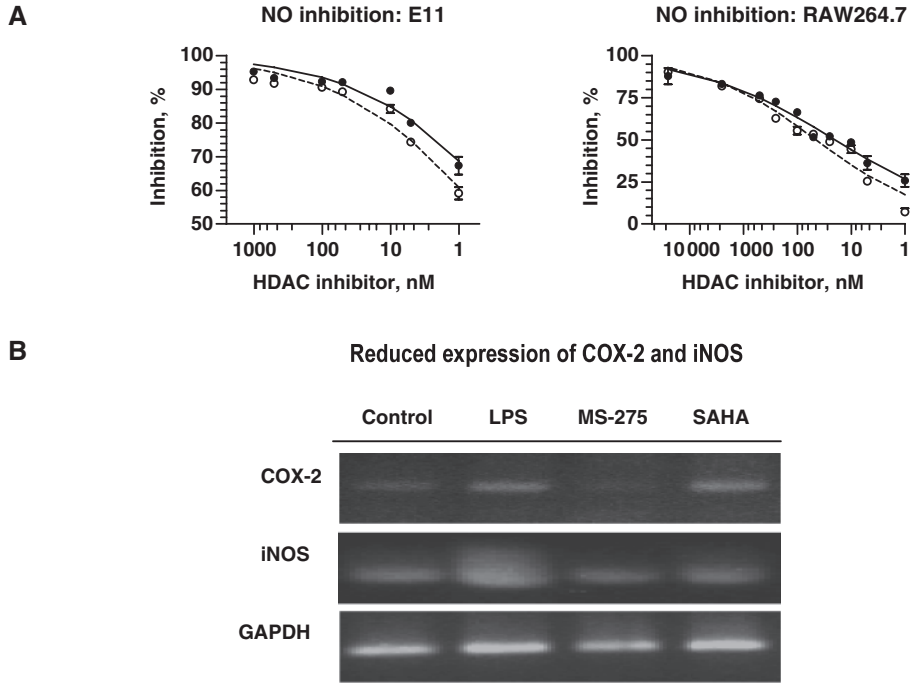

Relative densitometry

	LPS	MS-275	SAHA
COX-2	2.38	0.49	2.06
iNOS	1.88	0.68	0.95

FK-228, FR235222, MS-275, PB, SAHA and TSA have been reported in rodent models of RA [9–15].

The anti-rheumatic activities of HDAC inhibitors can be mediated by multiple mechanisms. Since tumour-like RASFs are characteristic players in RA [36], the anti-proliferative activities of HDAC inhibitors observed might help to combat RA. In the present study, MS-275 and SAHA significantly inhibited E11 cell proliferation with IC_{50} values <100 nM (MTT assay). Flow cytometry analyses indicated G_0/G_1 phase arrest. Such findings were in accordance with the previous studies carried out with FK-228 and TSA [9, 14]. FK-228 or TSA treatment also led to a phase arrest at G_0/G_1 with comparable potencies [9, 14]. Interestingly, we found that the growth inhibitory effects of MS-275 and SAHA (up to 25 μM) were independent of cytotoxicity in E11 cells. As also reported in previous studies, PB (up to 2 mM), TSA (up to 300 nM) and FK-228 (up to 100 nM) effectively inhibited RASF growth without causing cell death [9, 14]. However, we noticed that the inhibitory effect of MTX on E11 cell proliferation was accompanied with cytotoxicity. Even at 10 nM, MTX significantly elevated LDH activity in the media. Hence, the anti-proliferative mechanism of HDAC inhibitors appeared to be different from that of MTX. It might be of interest to note that the anti-cancer activities of HDAC inhibitors were often associated with their apoptotic effects [1, 2].

The anti-proliferative activities of HDAC inhibitors in RASFs could be mediated by the up-regulation of CDK inhibitors (p16 and p21). In eukaryotes, the cell cycle is regulated by the periodic synthesis and removal of cyclins that associate with and activate CDKs [26]. CDK inhibitors such as p16 and p21 are involved in cell cycle control by coordinating internal and external signals and impeding proliferation at several key checkpoints [26]. p16 or p21 dysfunction led to carcinogenesis, whereas up-regulation provided anti-cancer activities [1, 39–41]. HDAC inhibitors are well known for their ability to up-regulate the

FIG. 4 MS-275 and SAHA suppressed the secretion of IL-6, IL-18, VEGF and down-regulated MMPs in E11 cells. (**A**) E11 cells were incubated with MS-275 or SAHA at different concentrations for 24 h. IL-6 secretion was measured by ELISA ($n = 4$). (**B**) E11 cells were incubated with MS-275 or SAHA at different concentrations for 1 h. The secretion of IL-18 was stimulated by LPS. Twenty-four hours later, IL-18 secretion was measured by ELISA ($n = 4$). (**C**) E11 cells were incubated with MS-275 or SAHA at different concentrations for 1 h. The secretion of VEGF was stimulated by a combination of IL-6 (100 ng/ml), sIL-6R (100 ng/ml) and IL-1β (5 ng/ml). Twenty-four hours later, VEGF secretion was quantified by ELISA ($n = 4$). Predicted values (——), observed values (●) of MS-275 on pro-inflammatory cytokine and VEGF inhibition; predicted values (- - -), observed values (○) of SAHA on pro-inflammatory cytokine and VEGF inhibition. Bars show the mean (S.D.) in (**A–C**). (**D**) E11 cells were incubated with MS-275 or SAHA (100 nM) for 1 h. The secretion of MMPs was stimulated by LPS. The activities of MMP-2 and MMP-9 were assessed by gelatine zymography. Control: medium alone; LPS: LPS alone.

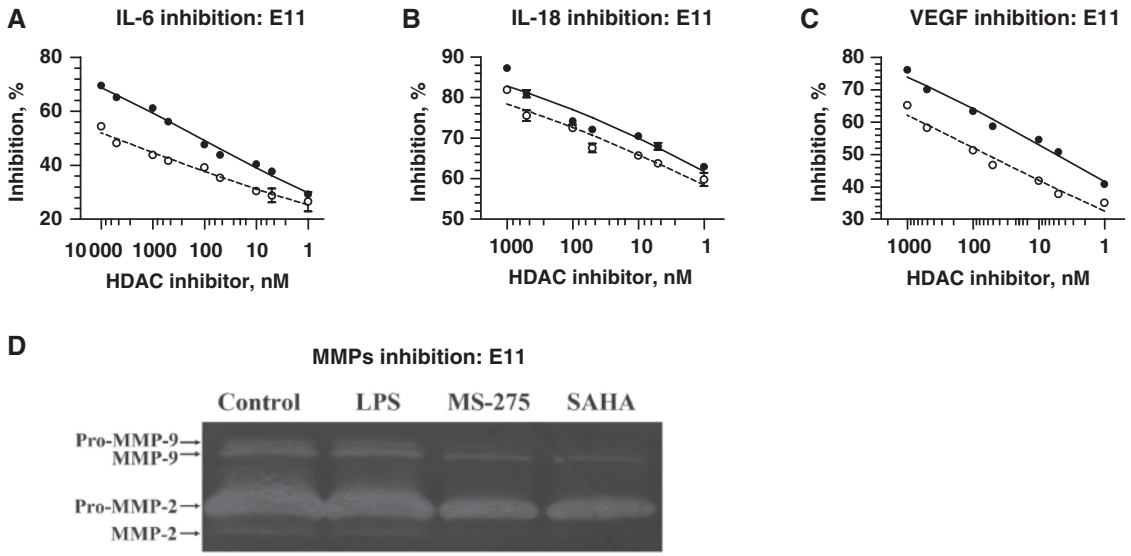

expression of CDK inhibitors (p16 or p21) in various types of cancer cells and this is one of their common anti-cancer mechanisms [1, 41].

Although the impact of p16 or p21 dysfunction on RA pathogenesis remains elusive, anti-rheumatic effects could be mediated through up-regulation of these genes. It was reported that forced expression of p16 or p21 by adenovirus transfection suppressed RASF proliferation [42–45], induced phase arrest at G_0/G_1 without cytotoxicity [43], inhibited the production of various inflammatory mediators and tissue-degrading enzymes such as IL-6, IL-8, IL-1R1, monocyte chemoattractant protein-1, macrophage inflammatory protein-3α, cathepsins B and K as well as MMP-1 and MMP-3 [43, 46]. Similar anti-proliferative activities were also observed with forced expression of p16 in RASFs [42, 44]. Moreover, gene therapy with p16 or p21 displayed good anti-rheumatic efficacy in rodent RA models [42, 44, 45]. Therefore, p16 or p21 up-regulation could provide a therapeutic strategy for RA.

HDAC inhibitors have been shown to be able to up-regulate the expression of p16 or p21 in RASFs. Chung *et al.* [9] reported that PB (2 mM) and TSA (200 nM) induced p16 and p21 expression in synovial cells isolated from AIA rats. TSA also up-regulated p21 in recent studies carried out with human RASFs [47–49]. FK-228 (10 nM) induced both p16 and p21 in human RASFs [14]. Similarly, we have also noticed the induction of p21 in E11 cells after incubation with 50 nM MS-275 or SAHA for 24 h. It could therefore be postulated that our observations, including cytotoxicity-independent proliferation inhibition, G_0/G_1 phase arrests as well as the down-regulation of pro-inflammatory cytokines and MMPs were consequences of p21 expression in RASFs. Hence, we believe that up-regulation of p21 can contribute to the anti-rheumatic activity of MS-275 and SAHA. Besides, up-regulation of CDK inhibitors (p16 and p21) appeared to be a common anti-rheumatic mechanism for the HDAC inhibitors.

The NF-κB signalling pathway has been well studied. Key NF-κB members include p50/p105 and p52/p100 dimers, RelA/p65, RelB and c-Rel [28]. NF-κB activation can occur via cytokine stimulation (canonical pathway), Toll-like receptors (non-canonical pathway) or DNA damage and other forms of stress, initiating a signalling pathway that converges on an enzyme complex containing two IκB kinases (IKKα and IKKβ) as well as a regulatory protein (IKKγ) that is required for IKK activation [28]. IKKs will phosphorylate IκBα at serine residues 32 and 36, which target the inhibitor for ubiquitination and degradation by the 26S proteosome [28].

FIG. 5 MS-275 and SAHA suppressed IL-1β, IL-6, IL-18 and TNF-α secretion in THP-1 cells. THP-1 cells were incubated with MS-275 or SAHA at different concentrations for 1 h. The secretion of pro-inflammatory cytokines was stimulated by LPS. Twenty-four hours later, cytokine levels were quantified by ELISA ($n = 4$). (**A**) IL-1β, (**B**) IL-6, (**C**) IL-18 and (**D**) TNF-α. Predicted values (——), observed values (•) of MS-275 on pro-inflammatory cytokine secretion; predicted values (- - -), observed values (○) of SAHA on pro-inflammatory cytokine secretion. Bars show the mean (S.D.) in (**A–D**).

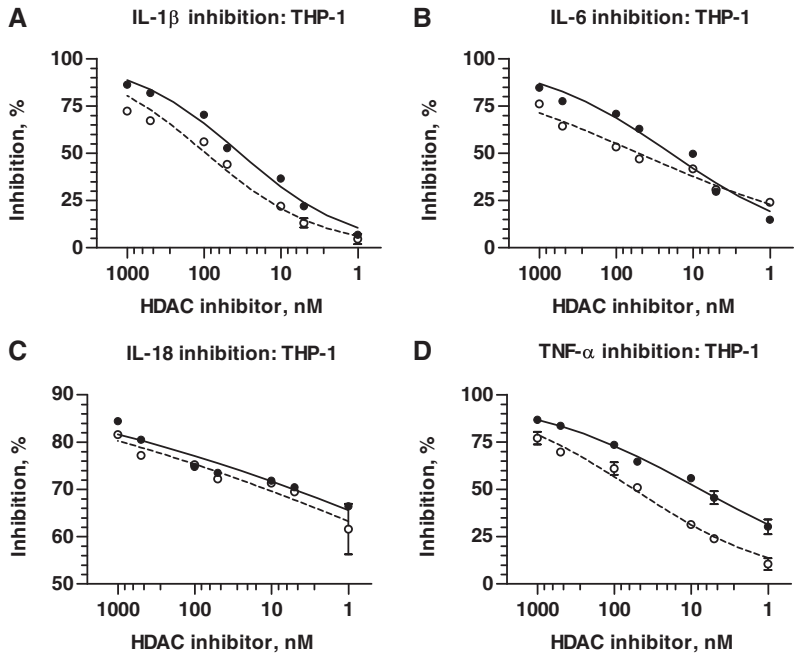

The anti-rheumatic mechanism for the HDAC inhibitors could also be mediated through inhibition of the NF-κB pathway. The transcriptional factor NF-κB is a pivotal regulator of inflammation in RA [27, 28]. NF-κB is activated in synovial tissues in the early stages of inflammation as well as in the late stages of disease [27]. As activation of NF-κB in SF profoundly enhances proliferation, motility and matrix-degrading activity, an essential role for NF-κB has been proposed in the tumour-like behaviour of RASFs [50]. Many pro-inflammatory genes involved in RA, such as IL-1, IL-6, TNF-α, COX-2, iNOS, VEGF and MMPs, are up-regulated after NF-κB activation in RA-related cells or tissues [50]. BAY 11-7082, a well-known NF-κB inhibitor, was found to suppress LPS-induced pro-inflammatory cytokine secretion in both E11 and THP-1 cells. Clearly, interruption of NF-κB pathway offers an anti-inflammatory strategy for RA [28, 51].

In this study, MS-275 and SAHA (100 nM) profoundly suppressed NF-κB p65 nuclear accumulation, an important step for NF-κB activation, in both E11 and THP-1 cells. To our knowledge, this is the first observation of inhibitory effects of HDAC inhibitor on NF-κB activation in RASFs. Furthermore, the levels for MS-275 and SAHA to display anti-rheumatic activities such as anti-proliferation, pro-inflammatory cytokines and iNOS suppression, angiogenesis inhibition and matrix-degradative enzyme down-regulation were within the levels in which NF-κB activation was inhibited. Inhibition of the NF-κB pathway appeared to be a common mechanism for HDAC inhibitors to display their anti-rheumatic activities in RA models.

The suppressive effect of HDAC inhibitors on NF-κB-mediated gene expression might be mediated through the inhibition of HDAC3. Kiernan *et al.* [52] reported that NF-κB p65 could be acetylated by p300 and de-acetylated by HDAC3. Acetylation on lysine residues 122 and 123 of p65 reduced its ability to bind κB-DNA and facilitated its removal from DNA and consequently its IκBα-mediated export from the nucleus [52]. Kiernan *et al.* [52] further proposed that acetylation of p65 plays a key role in IκBα-mediated attenuation of NF-κB transcriptional activity. Although MS-275 and SAHA enhanced the acetylation on NF-κB p65 lysine residue 310 (Fig. 2C), the acetylation status on other lysine residues was unknown due to the availability of the antibodies.

Our results appear to be well in line with such a theory. As MS-275 and SAHA effectively inhibit the HDACs, including HDAC3, acetylation on NF-κB p65 was enhanced. Subsequently, the acetylated NF-κB p65 could be removed to be exported into the cytoplasm (Fig. 2C) and become inactivated. As a result of the inhibition on NF-κB pathway, MS-275 and SAHA suppressed downstream transcription, leading to decreased

expression of iNOS and COX-2 and release of resultant MMPs, NO, pro-inflammatory cytokines and VEGF.

Noteworthy, in some other studies, acetylation on NF-κB p65 lysine residue 310 increased NF-κB-mediated gene expression [53–55]. Under such circumstances, HDAC worked as a suppressor for NF-κB-mediated gene expression [53–55]. Hence, HDAC inhibitors may work as pro-inflammatory agents instead. However, the effects of HDAC inhibitors on NF-κB activation are dependent on the cell type, stimulus and disease status [5]. The role of HDAC inhibitors in inflammatory diseases appeared to be double edged. In some airway and microglial inflammation, HDAC inhibitors worked as inflammatory enhancers; while in many other inflammatory conditions such as inflammatory bowel diseases, multiple sclerosis, RA and SLE, HDAC inhibitors displayed potent anti-inflammatory activity [5, 8].

MS-275 and SAHA exhibited their anti-rheumatic and anti-inflammatory activities with IC_{50} values mostly under 100 nM. However, their anti-cancer IC_{50} values were usually at μM levels [1, 2, 5]. Therefore, the dosages of MS-275 or SAHA used for RA may be lower than those used for oncology. Lower dosages can be a potential advantage to use HDAC inhibitors in the treatment of RA as dose-dependent side effects may be reduced. However, such a hypothesis needs to be tested in future clinical studies.

In summary, the anti-rheumatic activities of MS-275 and SAHA were mediated via inhibiting RASF proliferation, suppressing pro-inflammatory cytokine and NO release as well as down-regulating angiogenesis and MMPs. Their anti-rheumatic activities might possibly be attributed to the induction of CDK inhibitor p21 and suppression of the NF-κB pathway. Hence, HDAC inhibitors such as MS-275 and SAHA appeared to be a therapeutic strategy for RA.

Rheumatology key messages

- The anti-rheumatic activities of HDAC inhibitors might be attributed to induction of p21 and suppression of the NF-κB pathway.
- HDAC inhibitors such as MS-275 and SAHA can be therapeutic strategies for RA.

Acknowledgements

The authors would like to thank Mr Jia Yang for his technical assistance. Miss Qiu-Yi Choo is a recipient of a Research Scholarship from the National University of Singapore.

Funding: This study was supported by a research grant from Agency for Science, Technology and Research, Republic of Singapore (BMRC 06/1/21/19/441).

Disclosure statement: The authors have declared no conflicts of interest.

References

1 Johnstone RW. Histone-deacetylase inhibitors: novel drugs for the treatment of cancer. Nat Rev Drug Discov 2002;1:287–99.

2 Bolden JE, Peart MJ, Johnstone RW. Anticancer activities of histone deacetylase inhibitors. Nat Rev Drug Discov 2006;5:769–84.

3 Marks PA, Breslow R. Dimethyl sulfoxide to vorinostat: development of this histone deacetylase inhibitor as an anticancer drug. Nat Biotechnol 2007;25:84–90.

4 Grant S, Easley C, Kirkpatrick P. Vorinostat. Nat Rev Drug Discov 2007;6:21–2.

5 Choo QY, Ho PC, Lin HS. Histone deacetylase inhibitors: new hope for rheumatoid arthritis? Curr Pharm Des 2008; 14:803–20.

6 ClinicalTrials.gov. A service of the US National Institutes of Health. http://www.clinicaltrials.gov (15 January 2010, date last accessed).

7 Adcock IM. HDAC inhibitors as anti-inflammatory agents. Br J Pharmacol 2007;150:829–31.

8 Halili MA, Andrews MR, Sweet MJ, Fairlie DP. Histone deacetylase inhibitors in inflammatory disease. Curr Top Med Chem 2009;9:309–19.

9 Chung YL, Lee MY, Wang AJ, Yao LF. A therapeutic strategy uses histone deacetylase inhibitors to modulate the expression of genes involved in the pathogenesis of rheumatoid arthritis. Mol Ther 2003;8:707–17.

10 Nasu Y, Nishida K, Miyazawa S *et al*. Trichostatin A, a histone deacetylase inhibitor, suppresses synovial inflammation and subsequent cartilage destruction in a collagen antibody-induced arthritis mouse model. Osteoarthr Cartil 2008;16:723–32.

11 Mori H, Abe F, Furukawa S *et al*. Fr235222, a fungal metabolite, is a novel immunosuppressant that inhibits mammalian histone deacetylase (HDAC) ii. Biological activities in animal models. J Antibiot 2003;56:80–6.

12 Manabe H, Nasu Y, Komiyama T *et al*. Inhibition of histone deacetylase down-regulates the expression of hypoxia-induced vascular endothelial growth factor by rheumatoid synovial fibroblasts. Inflamm Res 2008;57:4–10.

13 Nakamura T, Kukita T, Shobuike T *et al*. Inhibition of histone deacetylase suppresses osteoclastogenesis and bone destruction by inducing IFN-beta production. J Immunol 2005;175:5809–16.

14 Nishida K, Komiyama T, Miyazawa S *et al*. Histone deacetylase inhibitor suppression of autoantibody-mediated arthritis in mice via regulation of p16ink4a and p21(waf1/cip1) expression. Arthritis Rheum 2004;50:3365–76.

15 Lin HS, Hu CY, Chan HY *et al*. Anti-rheumatic activities of histone deacetylase (HDAC) inhibitors in vivo in collagen-induced arthritis in rodents. Br J Pharmacol 2007;150:862–72.

16 Abe M, Tanaka Y, Saito K *et al*. Regulation of interleukin (IL)-1beta gene transcription induced by IL-1beta in rheumatoid synovial fibroblast-like cells, E11, transformed with simian virus 40 large t antigen. J Rheumatol 1997;24: 420–9.

17 Nakatsuka K, Tanaka Y, Hubscher S *et al*. Rheumatoid synovial fibroblasts are stimulated by the cellular adhesion to T cells through lymphocyte function associated

antigen-1/intercellular adhesion molecule-1. J Rheumatol 1997;24:458–64.

18 American Type Culture Collection. MTT cell proliferation assay instructions. http://www.Atcc.Org/portals/1/pdf/30-1010k.Pdf (15 January 2010, date last accessed).

19 Du YH, Ho PC. Arsenic compounds induce cytotoxicity and apoptosis in cisplatin-sensitive and -resistant gynecological cancer cell lines. Cancer Chemother Pharmacol 2001;47:481–90.

20 Ding AH, Nathan CF, Stuehr DJ. Release of reactive nitrogen intermediates and reactive oxygen intermediates from mouse peritoneal macrophages. Comparison of activating cytokines and evidence for independent production. J Immunol 1988;141:2407–12.

21 NIH. Imagej. http://rsbweb.Nih.Gov/ij/index.Html (15 January 2010, date last accessed).

22 Yoshifuji H, Umehara H, Maruyama H *et al*. Amelioration of experimental arthritis by a calpain-inhibitory compound: regulation of cytokine production by e-64-d in vivo and in vitro. Int Immunol 2005;17:1327–36.

23 Pierce JW, Schoenleber R, Jesmok G *et al*. Novel inhibitors of cytokine-induced IkappaBalpha phosphorylation and endothelial cell adhesion molecule expression show anti-inflammatory effects in vivo. J Biol Chem 1997;272:21096–103.

24 Garcia MG, Alaniz L, Lopes EC, Blanco G, Hajos SE, Alvarez E. Inhibition of NF-kappaB activity by Bay 11-7082 increases apoptosis in multidrug resistant leukemic T-cell lines. Leuk Res 2005;29:1425–34.

25 Nakahara H, Song J, Sugimoto M *et al*. Anti-interleukin-6 receptor antibody therapy reduces vascular endothelial growth factor production in rheumatoid arthritis. Arthritis Rheum 2003;48:1521–9.

26 Johnson DG, Walker CL. Cyclins and cell cycle checkpoints. Annu Rev Pharmacol Toxicol 1999;39:295–312.

27 Makarov SS. NF-kappa B in rheumatoid arthritis: a pivotal regulator of inflammation, hyperplasia, and tissue destruction. Arthritis Res 2001;3:200–6.

28 Firestein GS. NF-kappa B: holy grail for rheumatoid arthritis? Arthritis Rheum 2004;50:2381–6.

29 Roman-Blas JA, Jimenez SA. NF-kappaB as a potential therapeutic target in osteoarthritis and rheumatoid arthritis. Osteoarthr Cartil 2006;14:839–48.

30 McInnes IB, Schett G. Cytokines in the pathogenesis of rheumatoid arthritis. Nat Rev Immunol 2007;7:429–42.

31 Lee DM, Weinblatt ME. Rheumatoid arthritis. Lancet 2001;358:903–11.

32 Yoshihara Y, Nakamura H, Obata K *et al*. Matrix metalloproteinases and tissue inhibitors of metalloproteinases in synovial fluids from patients with rheumatoid arthritis or osteoarthritis. Ann Rheum Dis 2000;59:455–61.

33 Tchetverikov I, Ronday HK, van El B *et al*. MMP profile in paired serum and synovial fluid samples of patients with rheumatoid arthritis. Ann Rheum Dis 2004;63:881–3.

34 Huber LC, Brock M, Hemmatazad H *et al*. Histone deacetylase/acetylase activity in total synovial tissue derived from rheumatoid arthritis and osteoarthritis patients. Arthritis Rheum 2007;56:1087–93.

35 Horiuchi M, Morinobu A, Chin T, Sakai Y, Kurosaka M, Kumagai S. Expression and function of histone deacetylases in rheumatoid arthritis synovial fibroblasts. J Rheumatol 2009;36:1580–9.

36 Huber LC, Distler O, Tarner I, Gay RE, Gay S, Pap T. Synovial fibroblasts: key players in rheumatoid arthritis. Rheumatology 2006;45:669–75.

37 Firestein GS. Evolving concepts of rheumatoid arthritis. Nature 2003;423:356–61.

38 Mor A, Abramson SB, Pillinger MH. The fibroblast-like synovial cell in rheumatoid arthritis: a key player in inflammation and joint destruction. Clin Immunol 2005;115:118–28.

39 Sharpless NE, Bardeesy N, Lee KH *et al*. Loss of p16(INK4a) with retention of p19(ARF) predisposes mice to tumorigenesis. Nature 2001;413:86–91.

40 Martin-Caballero J, Flores JM, Garcia-Palencia P, Serrano M. Tumor susceptibility of p21(Waf1/Cip1)-deficient mice. Cancer Res 2001;61:6234–8.

41 Minucci S, Pelicci PG. Histone deacetylase inhibitors and the promise of epigenetic (and more) treatments for cancer. Nat Rev Cancer 2006;6:38–51.

42 Taniguchi K, Kohsaka H, Inoue N *et al*. Induction of the p16(INK4a) senescence gene as a new therapeutic strategy for the treatment of rheumatoid arthritis. Nat Med 1999;5:760–7.

43 Perlman H, Bradley K, Liu HT *et al*. IL-6 and matrix metalloproteinase-1 are regulated by the cyclin-dependent kinase inhibitor p21 in synovial fibroblasts. J Immunology 2003;170:838–45.

44 Nasu K, Kohsaka H, Nonomura Y *et al*. Adenoviral transfer of cyclin-dependent kinase inhibitor genes suppresses collagen-induced arthritis in mice. J Immunol 2000;165:7246–52.

45 Nonomura Y, Kohsaka H, Nasu K, Terada Y, Ikeda M, Miyasaka N. Suppression of arthritis by forced expression of cyclin-dependent kinase inhibitor p21(Cip1) gene into the joints. Int Immunol 2001;13:723–31.

46 Nonomura Y, Kohsaka H, Nagasaka K, Miyasaka N. Gene transfer of a cell cycle modulator exerts anti-inflammatory effects in the treatment of arthritis. J Immunol 2003;171:4913–9.

47 Morinobu A, Wang B, Liu J, Yoshiya S, Kurosaka M, Kumagai S. Trichostatin A cooperates with Fas-mediated signal to induce apoptosis in rheumatoid arthritis synovial fibroblasts. J Rheumatol 2006;33:1052–60.

48 Nakamura C, Matsushita I, Kosaka E, Kondo T, Kimura T. Anti-arthritic effects of combined treatment with histone deacetylase inhibitor and low-intensity ultrasound in the presence of microbubbles in human rheumatoid synovial cells. Rheumatology 2008;47:418–24.

49 Jungel A, Baresova V, Ospelt C *et al*. Trichostatin A sensitises rheumatoid arthritis synovial fibroblasts for trail-induced apoptosis. Ann Rheum Dis 2006;65:910–2.

50 Li X, Makarov SS. An essential role of NF-kappaB in the 'Tumor-like' phenotype of arthritic synoviocytes. Proc Natl Acad Sci USA 2006;103:17432–7.

51 Smolen JS, Steiner G. Therapeutic strategies for rheumatoid arthritis. Nat Rev Drug Discov 2003;2:473–88.

52 Kiernan R, Bres V, Ng RW *et al*. Post-activation turn-off of NF-kappa B-dependent transcription is regulated by acetylation of p65. J Biol Chem 2003;278:2758–66.

53 Spange S, Wagner T, Heinzel T, Kramer OH. Acetylation of non-histone proteins modulates cellular signalling at multiple levels. Int J Biochem Cell Biol 2009;41:185–98.

54 Greene WC, Chen LF. Regulation of NF-kappaB action by reversible acetylation. Novartis Found Symp 2004;259: 208–17, Discussion 18–25.

55 Chen LF, Greene WC. Regulation of distinct biological activities of the NF-kappaB transcription factor complex by acetylation. J Mol Med 2003;81:549–57.